

Population Controlled Impulsive Vibrational Spectroscopy: Background- and Baseline-Free Raman Spectroscopy of Excited Electronic States

*Torsten Wende, Matz Liebel, Christoph Schnedermann, Robert J. Pethick, and Philipp Kukura**

Physical and Theoretical Chemistry Laboratory, Department of Chemistry, University of Oxford,
South Parks Road, Oxford OX1 3QZ, United Kingdom

ABSTRACT

We have developed the technique of population controlled impulsive vibrational spectroscopy (pc-IVS) aimed at providing high-quality, background-free Raman spectra of excited electronic states and their dynamics. Our approach consists of a modified transient absorption experiment using an ultrashort (<10 fs) pump pulse with additional electronic excitation and control pulses. The latter allows for the experimental isolation purely excited state vibrational coherence and hence vibrational spectra. We illustrate the capabilities of pc-IVS by reporting the Raman spectra of well-established molecular systems such as the carotenoid astaxanthin and trans-stilbene and report the first excited state Raman spectra of the retinal protonated Schiff base chromophore in solution. Our approach, illustrated here with impulsive vibrational spectroscopy is equally applicable to transient and even multi-dimensional infrared and electronic spectroscopies to experimentally isolate the spectroscopic signatures of interest.

KEYWORDS Vibrational coherence, excited state Raman, ultrafast spectroscopy, retinal protonated Schiff base

INTRODUCTION

Time-resolved resonance Raman spectroscopy is an invaluable tool for the structural and kinetic characterization of excited electronic states in molecular systems.¹ A short, actinic, pump pulse generates a mixture of ground and excited state molecules that is subsequently probed with a second Raman pulse. When tuned in or near resonance with an electronic transition from an excited state, Raman scattering of electronically excited molecules is enhanced.² Time-energy uncertainty dictates a combined temporal and spectral resolutions on the order of a few picoseconds and few tens of cm^{-1} , respectively.³ The emergence of non-linear spectroscopies including coherent anti-stokes^{4,5} (CARS) and femtosecond stimulated Raman spectroscopies⁶⁻⁸ (FSRS) has recently challenged this limitation and especially the latter has been successful in recording ultrafast structural dynamics on both ground⁹ and excited¹⁰⁻¹¹ electronic states.

Despite these successes, several limitations remain that make routine acquisition of high-quality excited state Raman spectra challenging. Picosecond Raman spectroscopy requires long integration times and high incident powers¹² while struggling to achieve high spectral resolution ($<10 \text{ cm}^{-1}$) without significantly sacrificing both the efficient detection of Raman scattered photons and time-resolution. CARS struggles with interfering baselines¹³, which make identification of the desired Raman spectra difficult. For FSRS, off-resonant spectra appear almost invariably background free¹⁴, but large interfering baselines appear when tuning the Raman pulse near resonance.¹⁵ Therefore, one of the main advantages of Raman spectroscopy, resonance enhancement, has to be avoided due to the simultaneous amplification of unwanted alternative non-linear pathways.¹⁶ Additionally, the associated experimental setups are complex, as they involve a mixture of tunable femtosecond and picosecond pulses requiring sophisticated multi-stage optical parametric amplifiers.¹⁷⁻¹⁸ All techniques require manual subtraction of

ground state spectra, which is subjective and can be complex, in particular when ground and excited state spectra do not differ dramatically within the achievable spectral resolution. Similarly, accessing the low frequency region ($<200\text{ cm}^{-1}$) is challenging due to the spectral vicinity of the intense Raman pulse.

Here, we show that impulsive vibrational spectroscopy (IVS) in the time-domain^{8, 19-20} in combination with electronic population control²¹ is a powerful tool to obtain background-free excited state vibrational coherence (VC) and hence Raman spectra. To illustrate this, we will discuss the excited electronic state spectra of three molecular systems comprising the carotenoid astaxanthin (AXT), *trans*-stilbene (*t*SB) and *n*-butylamine retinal protonated Schiff base (nBu-RPSB). The first two systems represent well-established molecular benchmark systems and thus allow for an informative comparison with current frequency domain Raman techniques. The latter illustrates the power of population-controlled IVS (pc-IVS) by application to a molecular system that has proved to be prohibitively difficult to explore with the current state-of-the-art.

When combined with an actinic pump pulse^{8, 22-23}, IVS can be regarded as the time-domain equivalent to FSRS (**Figure 1a**). The experiment begins with an actinic pump promoting the molecule into an excited electronic state. After a time-delay T , a broadband pump-pulse, ideally resonant with an electronic transition from the excited state, impulsively generates VC on the excited electronic state. A time-delayed probe pulse then records the coherent evolution of the system in form of transient absorption (TA) spectra. In terms of an energy-ladder diagram, the light matter interactions leading to the eventually detected signal are identical to those for FSRS (**Figure 1b**), except that the electric fields are provided by different pulses. In the latter, the combination of a long Raman pump and a short Raman probe pulse generates the coherence, which is read out through a subsequent interaction with the Raman pump at any time before the

VC decays. The major advantage of the time-domain approach is that time- rather than frequency-domain probing of the VC reduces contributions of electronic, non-resonant signals that emerge in the same phase-matched direction as the desired signal. The only rapidly oscillating signatures that are recorded at longer time delays (>100 fs) are caused by nuclear wavepacket dynamics and provide background-free vibrational spectra after Fourier transformation.

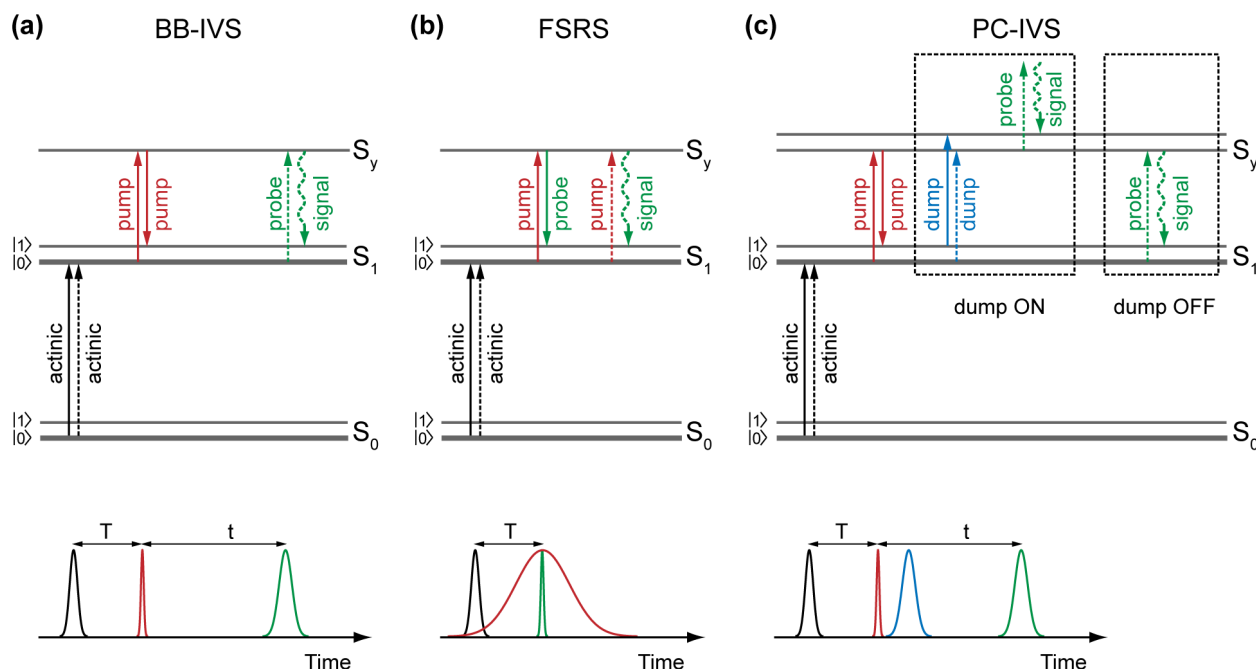


Figure 1. Wave mixing energy level (WMEL) diagrams of Raman spectroscopies for probing vibrational spectra of excited electronic states. **(a)** Broadband impulsive vibrational spectroscopy (BB-IVS). A three-pulse scheme records Raman spectra in the time-domain. The actinic pump pulse promotes molecules into the excited electronic state. After a fixed time delay T , a broadband pump pulse impulsively generates vibrational coherence (VC) on the excited electronic state. The evolution of the coherence is eventually probed by recording transient absorption (TA) spectra using a time-delayed probe pulse. **(b)** Femtosecond stimulated Raman spectroscopy (FSRS). VC is generated by the combination of a long Raman pump and a short

Raman probe pulse. The signal is read out by a second interaction with the Raman pump pulse during the vibrational dephasing time. (c) Population-controlled impulsive vibrational spectroscopy (pc-IVS). In the presence of a long (~ 200 fs) dump pulse resonant with an excited state transition (dump ON), some of the impulsively generated excited state coherences are projected onto another electronic state resulting in an overall reduced coherence activity on S_1 compared to the same experiment in the absence of the dump pulse (dump OFF). The long duration of the dump pulse ensures that the population of S_y is poorly time-resolved yielding no measurable time-varying signals. Comparison of experiments carried out in the presence and absence of the dump pulse thus allows for experimental isolation of excited state Raman activity.

A major disadvantage of IVS has been the stringent requirement on the achievable temporal resolution (< 20 fs) if VC is to be recorded over the entire spectral window of interest ($50 - 2000$ cm^{-1}) due to the associated short vibrational periods ($600 - 16$ fs). We recently showed such temporal resolutions are readily achievable using a combination of a moderately short (~ 12 fs) impulsive pump, compressed by commercially available chirped mirrors and a broadband, uncompressed white light continuum probe, which we termed broadband impulsive vibrational spectroscopy (BB-IVS).²² Our results demonstrated the high sensitivity of this technique to reveal VC on the excited electronic state of β -carotene and thereby the associated Raman spectrum. The broadband detection methodology furthermore revealed the spectral dependence of the VC and thereby, allowed for its assignment to its corresponding excited electronic state.

Irrespective of the technique, however, the isolation of pure excited state Raman spectra inevitably requires the removal of ground state and solvent contributions. Even if the impulsive pump pulse is tuned into resonance with an excited electronic state transition, there are many more ground state and solvent molecules in the probed region that will contribute to the overall

VC. In BB-IVS, the undesired contributions could be removed by applying an automated subtraction algorithm in the time domain²². However, as we will show in this study, the subtraction procedure is not always applicable but depends on the spectroscopic properties of the molecular system. In order to circumvent this limitation, we will present an alternative, experimental, approach based on electronic population control^{21, 24} to reveal excited state VC, which we refer to as pc-IVS (**Figure 1c**). The technique is similar to BB-IVS, but adds a fourth, longer-duration (>200 fs) dump pulse immediately following the impulsive pump, which is only resonant with excited state transitions and removes a fraction of the excited state population. Owing to its comparatively long temporal duration, the dump pulse cannot generate nuclear wavepackets (>75 cm⁻¹). Comparing experiments performed in the presence and absence of the dump pulse thus allows for the direct and purely experimental isolation of excited state Raman activity.

We remark that there are numerous other pathways potentially contributing to a signal emitted in the direction of the probe pulse²⁴, but found experimentally that pc-IVS signals are invariably dominated by excited state coherences when the dump pulse is resonant with a higher-lying excited electronic state and have thus restricted the discussion in Figure 1 to the most relevant WMEL diagrams. Our experiments are equivalent to those discussed in detail by Pollard and Mathies²⁵, except that an actinic pulse generates a mixture of ground and excited state molecules that is subsequently investigated by an impulsive pump-probe experiment. The further addition of a long-duration dump pulse that only affects excited state population and does not generate any measurable vibrational coherences leaving ground and solvent coherences unchanged.

EXPERIMENTAL SECTION

The experimental setup consists of an ultrafast amplifier source pumping a number of parametric amplifiers and a white light stage (**Figure 2a**). Four laser pulses are required to perform pc-IVS experiments. Actinic pump and dump pulses serve to electronically excite the molecules. Such pulses can be generated using a standard, tunable, optical parametric amplifier (OPA) or non-collinear OPA (NOPA), which commonly provide pulse durations on the order of 50 fs or shorter. A long-duration dump pulse (>200 fs) is convenient preventing the pulses from initiating VC (>75 cm^{-1}). Generation and recording of VC covering the entire fingerprint region of the molecule (<2000 cm^{-1}) requires impulsive pump pulses with temporal durations on the order of 10 fs which are readily obtained from a NOPA. Finally, an uncompressed white light probes the evolution of VC by recording TA spectra. The major advantage of this combination of pulses is that they are all easily producible from a femtosecond amplifier system. Pulses on the order of tens to a few hundred femtoseconds can be obtained from single-stage collinear OPAs or directly as harmonics of the laser fundamental, white light generation only requires a few standard optics and NOPAs have now become commonplace, including the previously elusive compression with chirped mirrors.

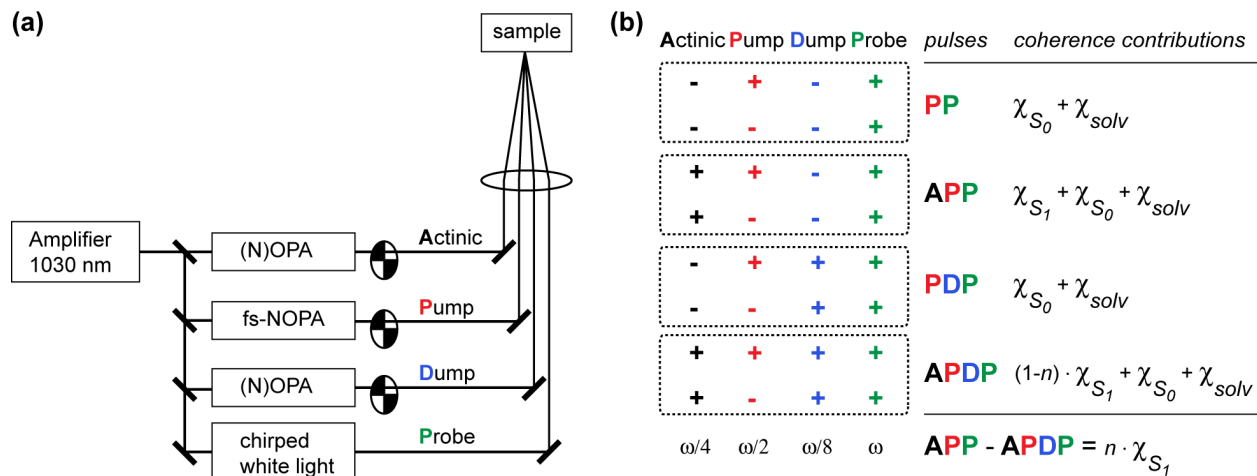


Figure 2. Population-controlled impulsive vibrational spectroscopy. (a) Schematic of the experimental setup. (b) Associated triple-chopping scheme and respective set of transient

absorption (TA) maps recorded in the experiment. Pump, actinic and dump beams are chopped with frequencies $\omega/2$, $\omega/4$ and $\omega/8$, respectively, where ω corresponds to the repetition rate of the probe beam (plus: ON, minus: OFF). Dashed boxes highlight four TA data sets that are simultaneously recorded. Each map differs in the amount of ground state (χ_{S0}), excited state (χ_{S1}) and solvent (χ_{Solv}) coherences. Comparison of the APP and APDP maps, recorded in the absence and presence of the dump pulse, respectively, isolates pure excited state Raman activity ($n \cdot \chi_{S1}$), where n corresponds to the fraction of excited state molecules which are removed by the interaction with the dump pulse.

In this work, laser pulses are delivered by a Pharos 6W amplifier (1030 nm, 180 fs, 5.5 W at 10 kHz). A single-stage white light-seeded OPA pumped at 515 nm provides pulses tunable in the near-infrared (NIR) region (700 – 950 nm) with pulse durations of ~ 200 fs. Frequency-doubling the OPA output conveniently extends the tuning range to 350 – 470 nm. Furthermore, the 1030 nm fundamental and its harmonics are additional sources of both actinic pump and dump pulses. The exact frequencies employed in each experiment are usually determined by the transient and stationary electronic spectra of the molecule of interest. For the impulsive pump pulse, we use a homebuilt white light-seeded NOPA in combination with commercially available chirped mirror compression (LAYERTEC) to obtain 10 fs pulses in either the visible or NIR spectral region.²⁶ A chirped white light (~ 300 fs, 2.5 nJ) serves as the probe, generated by focusing 1.5 μ J of the 1030 nm output into a 3 mm sapphire plate. Typical beam diameters applied in the sample area are 35 μ m (probe), 50 μ m (pump), 80 μ m (actinic) and 100 μ m (dump). The white light pulse covers a broad spectral range (500 – 900 nm) and thereby allows for simultaneously probing of multiple electronic transitions after excitation of the molecular

system. A home-built prism based spectrograph²⁷ equipped with a CMOS-array detector (LW-ELIS-1024A-1394) is used for broadband single shot detection at 10 kHz.

In terms of spectral selection, the actinic pump is chosen to coincide with the ground state absorption band of the system. The impulsive pulse, which is either in the visible or the NIR region, is tuned in resonance with an excited electronic state transition, such as excited state absorption (ESA) or stimulated emission (SE) bands, while avoiding spectral overlap with the ground state absorption region. The dump pulse spectrum is tuned spectrally to deplete excited electronic state population and temporally to arrive after the impulsive pump. Finally, the probe pulse ideally covers the broadest possible spectral range. With this combination of pulses, our pc-IVS experiments can be regarded as TA experiments with additional system preparation (actinic) and control (dump) pulses. We apply a triple-chopping scheme such that pump, actinic and dump beams are chopped with frequencies $\omega/2$, $\omega/4$ and $\omega/8$, respectively, where ω corresponds to the repetition rate of the probe beam and pump laser (**Figure 2b**). In this way, we are able to record a set of four different TA maps (dashed boxes, **Figure 2b**) that differ in the number of pulses involved, and hence, in the amount of VC contributions. We remark that the triple chopping scheme is chosen largely for convenience during alignment, a single chopping scheme alternating the dump pulse is, in principle, sufficient to record the desired data.

The pump-probe (PP) scheme represents the simplest case in which both actinic and dump beams are blocked. All molecules are in the electronic ground state (S_0), and since the impulsive pulse is non-resonant with the ground state absorption, the associated PP traces are dominated by ground state (χ_{S_0}) and solvent (χ_{solv}) VCs. In the actinic-pump-probe (APP) scheme, the actinic pump beam is unblocked and excites a subset of molecules into an excited electronic state (S_1). The corresponding APP traces additionally contain information about excited state Raman

activity (χ_{S1}). As demonstrated in BB-IVS, comparison of the PP to the APP map allows for the identification of excited state VCs and a subtraction algorithm often allows for the isolation of pure excited state VC, and hence Raman spectra.²² In the pump-dump-probe (PDP) scheme the dump beam is unblocked and the actinic beam is blocked. The same information is obtained as in the PP scheme, since the dump pulse is off-resonant and too long to generate any appreciable VC. In the actinic-pump-dump-probe (APDP) scheme both actinic and dump beam are unblocked which eventually enables us to experimentally isolate excited state Raman activity based on a comparison with the APP map. Both transients contain similar information about VC but differ slightly in the amount of excited state VC, since a small fraction of the excited state population is removed by the interaction with the dump pulse. Direct subtraction of the two data sets allows us to extract pure excited state VC activity.

All TA data is recorded by varying the time-delay between the impulsive pump and probe pulse. For each time-delay (t) the differential absorbance is obtained according to the following equation:

$$\Delta A = -\log_{10} \left(\frac{I_{ON}}{I_{OFF}} \right)$$

where I_{OFF} and I_{ON} correspond to the transmission spectra of the white light probe measured in the absence (*OFF*) and presence (*ON*) of the impulsive pump. The probed electronic signals are modulated by the oscillatory motion of the nuclear wavepacket and subtraction of the exponential electronic kinetics, based on a global fitting algorithm, isolates the VC. Fast Fourier transformation (FFT) of the oscillatory signal generates the time-domain Raman spectra as a function of the probe wavelength.^{21-22, 28} A single TA scan typically covers 2-3 ps sampled using a step size of 3.4 fs. The scan length is chosen such as to record the temporal evolution of VC while signal magnitudes remain sufficient, usually on the order of the vibrational dephasing time.

RESULTS AND DISCUSSION

BB-IVS: Time-domain Raman spectra of the S_1 state of AXT. BB-IVS in combination with computational subtraction allows for the removal of solvent and ground state coherences, which are always generated by the short impulsive pump if the following conditions are met. Firstly, tuning the broadband impulsive pump pulse in resonance with an ESA band significantly enhances the impulsive Raman process, which in turn enhances the generation of excited state VC. Secondly, in order to be able to subtract solvent contributions, characteristic solvent modes should be spectrally well-separated from ground and excited state vibrational modes. Carotenoid systems are well-suited to meet these requirements. Here we focus on the carotenoid AXT dissolved in dimethyl sulfoxide (DMSO) to illustrate the experimental strategy for recording and isolating excited state VC.

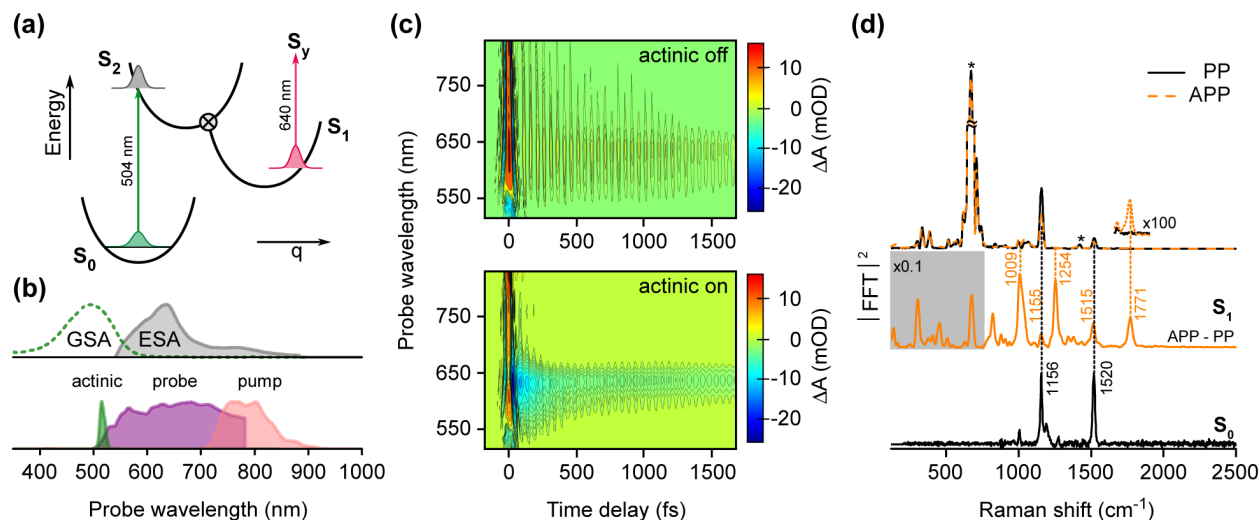


Figure 3. Broadband impulsive vibrational spectroscopy of astaxanthin. **(a)** Energy level scheme indicating the electronic transitions from the two lowest electronic singlet states. **(b)** Absorption (top) and pulse spectra (bottom) applied in the experiment. The actinic pump pulse (515 nm) is fully resonant with the ground state absorption. The broadband impulsive pump pulse is pre-

resonant with the absorption of the first excited electronic state. **(c)** Differential absorbance maps recorded in the absence (PP) and presence (APP) of the actinic pump pulse. **(d)** Fourier power spectra (top panel) obtained after globally fitting and subtracting the electronic kinetics. Raman spectra are averaged over the ESA region of the first excited electronic state (625 – 675 nm). Solvent bands (DMSO) are marked with an asterisk. The S_1 Raman spectrum (middle panel) is isolated by applying an automated subtraction algorithm to remove solvent and ground state contributions. The spectrum is compared to a continuous-wave ground state Raman spectrum (bottom panel).

Optical excitation with a 515 nm actinic pump pulse (~ 200 fs) promotes molecules from the ground (S_0) to the second excited singlet state (S_2). Fast internal conversion (~ 140 fs) transfers electronically excited molecules into the first excited state (S_1) which eventually decays back to S_0 with a 5 ps time constant (**Figure 3a**).²⁹ A corresponding differential absorbance spectrum of AXT in DMSO after internal conversion ($S_1 \leftarrow S_2$) exhibits a characteristic S_1 ESA signal at 640 nm (**Figure 3b**). From an ensemble perspective, the actinic pump pulse has generated a mixture of molecules in the S_0 and S_1 electronic states. The pulse energy of the actinic pump (20 nJ) has been adjusted to excite 25% of the molecules into the S_2 state. To record VC of the S_1 state, the impulsive pump pulse (~ 10 fs, centered at 800 nm, 20 nJ) arrives after a fixed time delay of 1 ps. The impulsive pump pulse is pre-resonant with the $S_y \leftarrow S_1$ and off-resonant with the $S_2 \leftarrow S_0$ electronic transition (**Figure 3b**).

Our spectral observation window specifically probes the region of the S_1 excited state absorption. The APP map is therefore dominated by the S_1 bleach signal around 640 nm, which is absent in the PP map (**Figure 3c**). Both TA maps differ in the amount and the nature of generated VC, as can be understood by considering the following equations:

$$VC_{PP} = \chi_{S_0} + \chi_{DMSO}$$

$$VC_{APP} = a \cdot \chi_{S_0} + b \cdot \chi_{DMSO} + \chi_{S_1}$$

where the S_0 , S_1 and solvent VC contributions are described by χ_{S_0} , χ_{S_1} and χ_{DMSO} , respectively. In the PP map only ground state and solvent molecules contribute to the VCs with an intensity dependence that scales with the derivative of the ground state absorption spectrum.⁸ In the APP map, VC from excited state molecules also contributes. Following FFT and averaging over the S_1 ESA region (630 – 670 nm) yields the respective Raman spectra (**Figure 3d**, top panel). Both spectra are dominated by the large Raman activity of DMSO resulting in an intense band at 670 cm^{-1} and a weaker band at 1420 cm^{-1} . Characteristic S_0 bands are observed at 1156 cm^{-1} and 1520 cm^{-1} . The corresponding Raman amplitudes are slightly reduced in the APP Raman spectrum, indicating the removal of ground state molecules by the interaction with the actinic pump. In addition, new Raman features appear in the APP Raman spectrum, which we associate with excited state Raman activity. Specifically, we observe a peak at 1771 cm^{-1} representing a marker band (C=C stretching) of the S_1 state in carotenoids.³⁰

In order to isolate the pure excited state VC, and hence the S_1 Raman spectrum, an efficient subtraction methodology is required. In general, it would be desirable to simply compute the difference of the VC, i.e. $VC_{APP} - VC_{PP}$. However, this procedure is not applicable since both maps differ in the amount of generated S_0 and solvent coherences (see equations above). However, a subtraction algorithm²² enables us to isolate the desired S_1 VC based on a two-step approach. Briefly, if the pure solvent and ground state coherences are known, the algorithm can remove these contributions by scaling the amplitude and phase of the corresponding oscillations. Thus, we first extract pure solvent VC by recording a TA map of neat DMSO. The spectral regions around 670 cm^{-1} and 1420 cm^{-1} are characteristic of DMSO, and we use these regions to

optimize the subtraction parameters and ultimately eliminate solvent contributions from both the PP and APP maps. Removal of solvent VC from the PP map results in a map that contains pure S_0 VC. This map serves as a reference to subtract the residual S_0 VC from the APP map. Here, we focused on the spectral region around 1156 and 1520 cm^{-1} for optimizing the subtraction parameters.

The dominant appearance of the DMSO and S_0 bands are efficiently removed in the isolated S_1 spectrum (**Figure 3d**, middle panel). Instead, four bands dominate the fingerprint region (750 – 2000 cm^{-1}), including the C=C stretch at 1771 cm^{-1} as well as features at 1254 cm^{-1} (C-C), 1009 cm^{-1} and 822 cm^{-1} . Furthermore, the S_1 spectrum reveals bands at 1155 cm^{-1} and 1515 cm^{-1} , which are weaker in intensity. The latter band is assigned to the C=C stretching motion and appears slightly red-shifted (-5 cm^{-1}) with respect to the S_0 band (**Figure 3c**, bottom panel).

In summary, application of BB-IVS in combination with computational removal of residual S_0 and solvent coherences allows us to retrieve a high-quality excited state Raman spectrum of AXT. The method highly benefits from the fact that the ESA is spectrally well-isolated from any other electronic transitions. In this way, it ensures that no population transfer contributes to the generation of VCs thus leading to very reliable performance of the subtraction algorithm.

BB-IVS vs pc-IVS: Excited state coherence in nBu-RPSB. The subtraction of residual ground state VC becomes particularly challenging if population transfer from the excited to the ground electronic state is involved during the generation of VC. Here we focus on nBu-RPSB as an example to (a) demonstrate the breakdown of computational subtraction of ground state and solvent VC, and (b) to motivate and introduce an experimental subtraction scheme based on electronic population control.

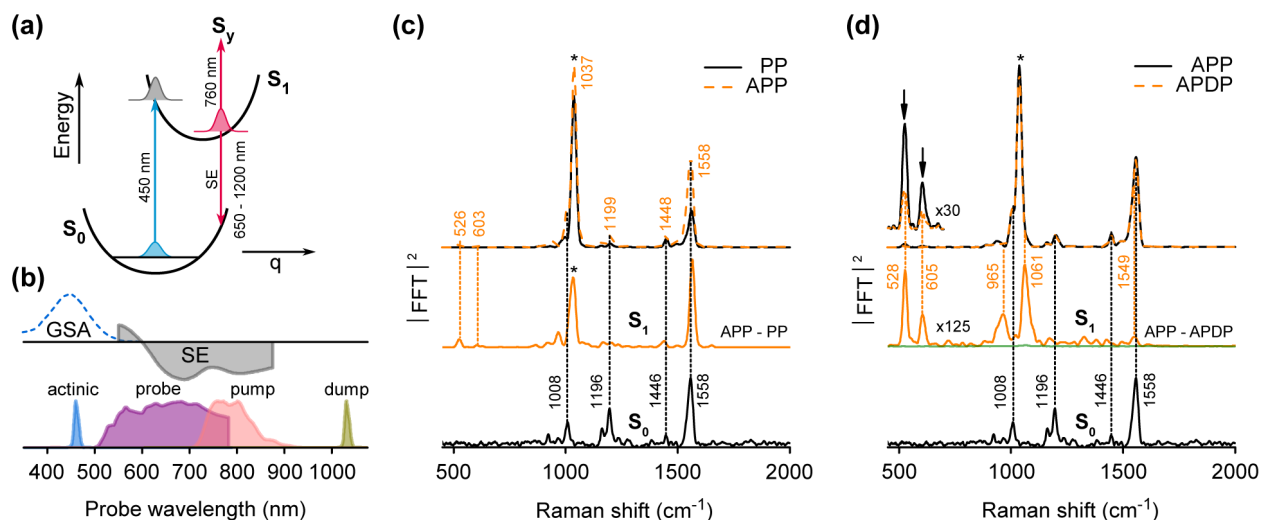


Figure 4. Impulsive vibrational spectroscopy of retinal protonated Schiff base in solution. **(a)** Energy level scheme indicating the electronic transitions of the two lowest electronic singlet states. **(b)** Absorption (top) and pulse spectra (bottom) applied in the experiment. A characteristic stimulated emission band (SE) is observed in the region >600 nm, which spectrally overlaps with an excited state absorption peaking at 760 nm. The blue dashed line represents the ground state absorption spectrum. **(c)** BB-IVS in combination with a subtraction algorithm. Top: Fourier power spectra before application of the subtraction algorithm. Raman spectra are averaged over the S_1 SE band (745 – 830 nm). Solvent bands (MeOH) are marked with an asterisk. Middle: Fourier power spectrum after application of the subtraction algorithm. Bottom: Continuous-wave Raman spectrum of nBu-RPSB in MeOH. **(d)** PC-IVS for direct isolation of S_1 Raman activity. Top: Fourier power spectra recorded in the absence (APP) and presence (APDP) of the dump pulse. Middle: Isolated S_1 Raman spectrum. Spectral contributions originating from the dump pulse interaction were isolated (green solid trace) by comparing PP and PDP maps. Bottom: Continuous-wave ground state Raman spectrum of nBu-RPSB in MeOH.

The ground state absorption of nBu-RPSB in methanol (MeOH) has a maximum at 450 nm (Figure 4a, b). We therefore use a 450 nm actinic pump pulse (~ 200 fs, 300 nJ) in order to

excite 25% of the molecules into the S_1 state. The S_1 ESA and SE bands are overlapping (650 - 1200 nm) leading to a characteristic double-hump feature in the differential absorbance spectrum (**Figure 4b**).³¹ As we will show in the following, the presence of an often encountered stimulated emission band makes it impossible to use the BB-IVS scheme in order to isolate excited state VCs. We employ a near-infrared impulsive pump (~10 fs, centered at 800 nm, 90 nJ) resonant with both the SE and ESA transitions. The following equations describe the various VC contributions (χ_i) generated in the absence (VC_{PP}) and presence (VC_{APP}) of the actinic pump pulse:

$$VC_{PP} = \chi_{S0} + \chi_{MeOH}$$

$$VC_{APP} = a \cdot \chi_{S0} + \chi_{S0}^{SE} + b \cdot \chi_{MeOH} + \chi_{S1}$$

In the PP scheme, both ground state (χ_{S0}) and solvent VC (χ_{MeOH}) are off-resonantly created by stimulated Raman scattering. In contrast, after optical excitation to the S_1 state by the actinic pump, SE introduces an additional pathway to generate S_0 VC. More specifically, the impulsive pump not only enhances the generation of S_1 VC (χ_{S1}) but also efficiently enhances the generation of ground state nuclear wavepackets (χ_{S0}^{SE}) via the SE transition from the S_1 into the S_0 state. Similar conditions are, for instance, responsible for complex lineshapes and strong ground state interferences in FSRS.¹⁶ In addition to the overall scaling, changes in the excited to ground state displacements will lead to differences in the relative band intensities, making any subtraction difficult.

Under the present experimental conditions, coherent oscillations with signal magnitudes of about 3 mOD at 790 nm are initially recorded at early pump-probe delays, i.e. 200 fs after generation of VC by the pump. The associated Raman spectra of both PP and APP maps are dominated by an intense band at 1037 cm^{-1} , which is characteristic of MeOH (**Figure 4c**, top

panel). The higher frequency region exhibits three bands at 1558, 1448 and 1199 cm^{-1} , associated with ground state vibrational modes. Interestingly, the respective band intensities increase in the presence of the actinic pulse with the 1558 cm^{-1} band being particularly affected. This observation can be explained by considering that S_0 VC is very efficiently generated by SE from S_1 .

The subtraction algorithm for removing residual solvent and S_0 VC results in a Raman spectrum that still contains the 1037 cm^{-1} MeOH band as well as the 1558 cm^{-1} S_0 mode as dominant features (**Figure 4c**, middle panel). This observation confirms that the subtraction algorithm is not applicable in this case. The breakdown of the computational subtraction can be mainly attributed to the following two aspects. Firstly, the quality of the solvent subtraction suffers from the fact that the intense MeOH band spectrally overlaps with ground state vibrational modes emerging around 1000 cm^{-1} . As the solvent contributions are strongest in that spectral region, we select this specific range to optimize the subtraction. However, the presence of S_0 VC introduces a significant error in the phase optimization of the subtraction algorithm, which results in residual MeOH features after subtraction. Secondly, subtraction of S_0 VC suffers from the fact that the PP and APP maps contain S_0 VC contributions that were generated by different mechanisms. The PP map lacks information about VC contributions which are generated via SE (see equations above) and satisfactory S_0 subtraction from the APP map is thus elusive. The solvent subtraction could be improved by using a different solvent whose vibrational modes are spectrally well-separated from characteristic S_0 modes of the solute. However, subtraction of S_0 VC can only be improved by tuning the impulsive pump out of the SE region, which is not feasible for many molecular systems either because the pulses are not

available or because, as for nBu-RPSB, such regions do not exist within the UV-NIR spectral range.

By addition of a long-duration dump pulse for electronic population control it becomes, however, possible to isolate pure S_1 VC. Specifically, we use a 1030 nm pulse (~ 200 fs, 230 nJ) that overlaps with the low-energy tail of the SE band removing 20% of the excited state population (**Figure 4b**). One key aspect of pc-IVS is that the dump pulse is applied after VC has been generated by the impulsive pump pulse. Owing to its long pulse duration (>200 fs) population control removes excited state population via SE without generating VC (>75 cm^{-1}). The depletion of excited state population will be reflected in a reduction of excited state VC, and hence, a decrease in the Raman intensities. Comparison of the TA maps recorded in the absence (APP) and presence of the dump pulse (APDP) directly isolates the VC of the excited state, as described by the following equations:

$$\begin{aligned} VC_{APP} &= \chi_{S0} + \chi_{S0}^{SE} + \chi_{MeOH} + \chi_{S1} \\ VC_{APDP} &= \chi_{S0} + \chi_{S0}^{SE} + \chi_{MeOH} + (1 - n) \cdot \chi_{S1} \\ VC_{APP-APDP} &= n \cdot \chi_{S1} \end{aligned}$$

Here, $VC_{APP-APDP}$ corresponds to the difference of the signals recorded in the APP and APDP maps, with n being the fraction of molecules removed from the excited state by the action of the dump pulse.

Direct comparison of the Raman spectra retrieved from the APP and APDP maps reveals only subtle differences in the observed Raman band intensities (**Figure 4d**, top panel). For example, we observe an intensity reduction for the vibrational modes at 528 and 605 cm^{-1} , indicating that these are characteristic S_1 signatures. In the higher frequency region, changes in the band

intensities are small and hardly resolved at this stage of the analysis, especially because the spectra are still dominated by S_0 and solvent VC.

In contrast, direct subtraction of the APP from the APDP map in the time-domain isolates the S_1 Raman activity, indicated by the efficient removal of both MeOH and S_0 features as for example at 1037 and 1558 cm^{-1} (**Figure 4d**, middle panel). The pc-IVS results are significantly different from the spectrum obtained by BB-IVS. Four new Raman features dominate the isolated S_1 spectrum, two low-frequency modes at 528 and 605 cm^{-1} as well as modes at 965 and 1061 cm^{-1} . In fact, the ring deformation modes near 600 cm^{-1} are the clearest indicator of the efficiency and importance of the pump-dump scheme. These bands are almost invisible in the raw spectra, but the comparison of APP and APDP spectra shows that they originate from the excited state. This assignment is confirmed by the final S_1 spectrum, in addition to a series of other bands that would have been impossible to identify from the raw spectra alone.

For a reliable isolation of pure excited state VC it is essential that the presence of the dump pulse does not perturb the S_0 and solvent VC. Comparison of PP and PDP Raman spectra allows us to directly retrieve spectral changes that originate from the dump pulse interaction. Under the present experimental conditions, the changes in coherent intensities of ground and solvent coherences caused by the dump pulse (center panel, Figure 4d) are two orders of magnitudes smaller compared to excited state coherences, showing that spectral distortions by the dump pulse are negligible.

In summary, pc-IVS avoids the difficulties encountered with the computational subtraction of solvent and S_0 VC. Although the implementation of a dump pulse adds experimental complexity, electronic population control facilitates an experimental subtraction scheme that allows us to directly retrieve background-free excited state Raman spectra, regardless of the pathways that

contribute to the generation of VC. As demonstrated on nBu-RPSB, the technique allows us to extend vibrational studies toward molecules that have so far been inaccessible by state-of-the-art Raman spectroscopies due to their specific electronic resonances.

pc-IVS vs FSRS: Excited state coherence in *t*SB. The excited state Raman spectra of *t*SB have been extensively studied both experimentally and theoretically.^{7-8, 11, 17, 32} This molecule thus forms an ideal benchmark system to compare our time-domain approach to current state-of-the-art frequency-domain techniques. More specifically, we will focus on a comparison between FSRS and pc-IVS. In their recent FSRS study Dobryakov et al.¹¹ reported very high-quality ground and excited state spectra of *t*SB in *n*-hexane (**Figure 5a**). The S_1 Raman spectrum contains a rich number of Raman bands in the 100-1700 cm^{-1} region, with the most intense bands emerging at 285, 1181, 1241 and 1568 cm^{-1} . The typical spectral resolution of the S_1 modes is 20 cm^{-1} , limited by the vibrational dephasing of excited-state coherences, estimated by the authors to occur roughly within 1 ps, as well as the spectral resolution of the detection system.

For optical excitation ($S_1 \leftarrow S_0$) we use a 250 fs actinic pump pulse centered at 325 nm (60 nJ). Specifically, we use a sample solution of OD = 0.8 and adjusted the actinic pump power to be in the linear regime. A visible pump pulse (9 fs, centered at 550 nm, 30 nJ) which is fully resonant with the S_1 ESA band ($\lambda_{\text{max}} = 580 \text{ nm}$)¹¹ efficiently generates VC on the S_1 state 2 ps after photoexcitation. Isolation of the S_1 VC is achieved by applying a 515 nm dump pulse (~200 fs, 160 nJ) which is only resonant with the S_1 ESA band. The dump power was adjusted such that 20% of the S_1 population is removed via ESA. The temporal evolution of the VCs was recorded over 4.8 ps thus covering the full vibrational dephasing of the excited-state wavepackets and hence allowing for the highest possible spectral resolution.

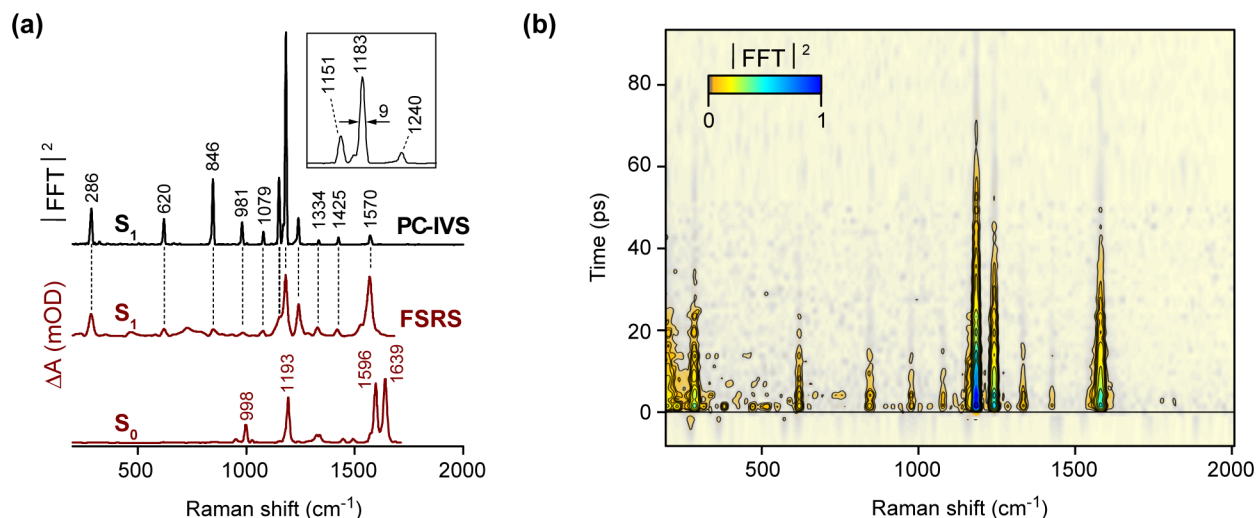


Figure 5. pc-IVS on *trans*-stilbene (*t*SB). **(a)** Isolated S_1 Raman spectrum (top panel) of *t*SB in *n*-hexane averaged over the ESA region (540 – 690 nm). The inset (upper right) covers the region from 1100 to 1290 cm^{-1} . Corresponding APP and APDP maps were sampled over the vibrational dephasing time (4.8 ps) to obtain the highest possible spectral resolution (FWHM: $<15 \text{ cm}^{-1}$). pc-IVS results are compared with FSRs spectra (lower panels) of ground (S_0) and excited electronic state (S_1) previously reported by Dobryakov et al.¹¹. **(b)** Time-resolved pc-IVS spectra *t*SB in toluene. The intensity plot comprises 150 time points sampling 100 ps after photoexcitation. For each time step a single spectrum was recorded within 25s.

The isolated S_1 Raman spectrum (**Figure 5a**, top panel) is dominated by 11 characteristic Raman bands in excellent agreement with the FSRs results. Moreover, PC-IVS yields a Raman spectrum with unprecedented spectral resolution resulting in a typical bandwidth of $<15 \text{ cm}^{-1}$ (FWHM). For example, the most intense Raman band observed at 1183 cm^{-1} exhibits a linewidth of 9 cm^{-1} (inset, **Figure 5a**). The resulting TA map obtained after direct subtraction of the APP from the APDP map contains pure S_1 coherences which are retrieved by globally fitting the electronic kinetics and subsequent subtraction. Beyond that, no complex data analysis, i.e. no

subtraction of ground state or solvent features nor any correction for non-trivial line shapes or baselines, is needed to retrieve the excited state Raman spectra.

Despite the excellent agreement in peak positions between pc-IVS and FSRS, there are clear differences in the band intensities. In general, we find that the band intensities vary strongly with the detection wavelength and the relative band position of the excited state electronic transition. We therefore usually average over the entire band where possible, in this case 540 – 690 nm) to avoid any bias. Nevertheless, this is an aspect of pc-IVS that remains to be explored in more detail both experimentally and theoretically in the future and work in this regard is currently underway. We remark, however, that even small changes in Raman illumination wavelength can lead to drastic changes in relative peak intensities as demonstrated recently by Ernsting and coworkers.^{7,11}

In order to highlight the full potential of the developed technique, we varied the time delay between the actinic and the impulsive pump pulses, which enables us to record time-resolved Raman spectra of the S_1 state. We recorded S_1 Raman spectra for 150 time points thereby sampling the first 100 ps after photoexcitation. To ensure long-term signal stabilities we, however, switched the solvent from n-hexane to the less volatile toluene. All other experimental parameters were kept as outlined previously. At each time point a single spectrum was recorded within 25 s. Taking advantage of electronic population control, we are able to monitor the structural dynamics with high sensitivity as the molecule decays back to S_0 , as reflected by a decrease in Raman band intensities (**Figure 5b**). Our time-dependent data show a slow change in Raman intensities over the first 10 ps in contrast to previous FSRS studies⁷ where a rapid decrease in intensity is observed within the first picosecond. The latter is most likely attributed to rapid vibrational cooling of internally hot S_1 molecules, thus changing the involved Raman cross-

sections, possibly due to large changes in resonance enhancement. While a 280 nm actinic pump pulse is applied in the FSRS studies, our pc-IVS experiment uses 325 nm excitation which results in much lower internal energy of S1 molecules, and leads only to minor cooling effects. This observation is supported by TA experiments by Kovalenko et al.³³ showing that 325 nm excitation leads to excited state molecules at $T = 294$ K while bluer excitation using a 267 nm pulse results in excited state molecules with much higher internal energies corresponding to $T = 600$ K.

Given the high signal-to-noise ratio achieved it should be possible to further decrease the integration time. We are currently, however, limited by the maximum stepping rate of our translation stage. A reduction of the total experimental time for acquiring 150 time points, from 60 mins to well below 10 mins, should be in reach in the near future.

CONCLUSIONS

We have shown that the combination of time-domain impulsive vibrational spectroscopy with electronic population control (pc-IVS) represents a powerful tool for recording pure excited state Raman spectra in the time-domain. The addition of a dump pulse facilitates the direct, experimental isolation of excited state vibrational coherences and retrieval of baseline free Raman spectra. The experimental subtraction scheme avoids the often subjective removal of both ground state and solvent signatures. Importantly, probing of vibrational coherences and thus Raman spectra natively takes advantage of resonance enhancement, one of the most useful aspects of Raman spectroscopy. Together with the simple experimental approach compared to current state-of-the-art frequency-domain techniques and the high achievable signal-to-noise ratios, pc-IVS has the potential of providing unique new insights into chemical reaction

dynamics. Beyond applications to Raman spectroscopy, the addition of a pulse capable of specifically modifying the population of a particular electronic state in a non-perturbative fashion for all other species is a general route to experimental isolation of desired spectroscopic signatures.

AUTHOR INFORMATION

Corresponding Author

* Address correspondence to philipp.kukura@chem.ox.ac.uk

Author Contributions

The manuscript was written through contributions of all authors. All authors have given approval to the final version of the manuscript.

Funding Sources

-

Notes

-

ACKNOWLEDGMENT

This research was supported by an EPSRC career acceleration fellowship (EP/H003541/1), an EPSRC standard grant (EP/K006630/1) and by a Marie Curie Intra European Fellowship (PIEF-GA-2013-623652) within the 7th European Community Framework Programme.

REFERENCES

- (1) Hamaguchi, H.; Gustafson, T. L. Ultrafast Time-Resolved Spontaneous And Coherent Raman Spectroscopy: The Structure and Dynamics of Photogenerated Transient Species. *Annu. Rev. Phys. Chem.* **1994**, *45*, 593-622.
- (2) Kim, J. E.; McCamant, D. W.; Zhu, L.; Mathies, R. A. Resonance Raman Structural Evidence that the Cis-to-Trans Isomerization in Rhodopsin Occurs in Femtoseconds. *J. Phys. Chem. B* **2001**, *105*, 1240-1249.
- (3) Wang, C.; Tauber, M. J. High-yield Singlet Fission in a Zeaxanthin Aggregate Observed by Picosecond Resonance Raman Spectroscopy. *J. Am. Chem. Soc.* **2010**, *132*, 13988-13991.
- (4) Tolles, W. M.; Nibler, J. W.; McDonald, J. R.; Harvey, A. B. Review of Theory and Application of Coherent Anti-stokes Raman-Spectroscopy (CARS). *Appl. Spectrosc.* **1977**, *31*, 253-271.

- (5) Schmitt, M.; Knopp, G.; Materny, A.; Kiefer, W. Femtosecond Time-Resolved Coherent Anti-Stokes Raman Scattering for the Simultaneous Study of Ultrafast Ground and Excited State Dynamics: Iodine Vapour. *Chem. Phys. Lett.* **1997**, *270*, 9-15.
- (6) Kukura, P.; McCamant, D. W.; Mathies, R. A. Femtosecond Stimulated Raman Spectroscopy. *Annu. Rev. Phys. Chem.* **2007**, *58*, 461-88.
- (7) Weigel, A.; Ernsting, N. P. Excited Stilbene: Intramolecular Vibrational Redistribution and Solvation Studied by Femtosecond Stimulated Raman Spectroscopy. *J. Phys. Chem. B* **2010**, *114*, 7879-7893.
- (8) Takeuchi, S.; Ruhman, S.; Tsuneda, T.; Chiba, M.; Taketsugu, T.; Tahara, T. Spectroscopic Tracking of Structural Evolution in Ultrafast Stilbene Photoisomerization. *Science* **2008**, *322*, 1073-7.
- (9) Kukura, P.; McCamant, D. W.; Yoon, S.; Wandschneider, D. B.; Mathies, R. A. Structural Observation of the Primary Isomerization in Vision with Femtosecond-Stimulated Raman. *Science* **2005**, *310*, 1006-9.
- (10) Fang, C.; Frontiera, R. R.; Tran, R.; Mathies, R. A. Mapping GFP Structure Evolution during Proton Transfer with Femtosecond Raman Spectroscopy. *Nature* **2009**, *462*, 200-204.
- (11) Dobryakov, A. L.; Ioffe, I.; Granovsky, A. A.; Ernsting, N. P.; Kovalenko, S. A. Femtosecond Raman Spectra of Cis-Stilbene and Trans-Stilbene with Isotopomers in Solution. *J. Chem. Phys.* **2012**, *137*, 244505-244516.
- (12) Deak, J. C.; Iwaki, L. K.; Dlott, D. D. Vibrational Energy Redistribution in Polyatomic Liquids: Ultrafast IR-Raman Spectroscopy of Acetonitrile. *J. Phys. Chem. A* **1998**, *102*, 8193-8201.
- (13) Atkinson, G. H.; Ujj, L.; Zhou, Y. Vibrational Spectrum of the J-625 Intermediate in the Room Temperature Bacteriorhodopsin Photocycle. *J. Phys. Chem. A* **2000**, *104*, 4130-4139.
- (14) McCamant, D. W.; Kukura, P.; Yoon, S.; Mathies, R. A. Femtosecond Broadband Stimulated Raman Spectroscopy: Apparatus and Methods. *Rev. Sci. Instrum.* **2004**, *75*, 4971-80.
- (15) Kukura, P.; McCamant, D. W.; Mathies, R. A. Femtosecond Time-Resolved Stimulated Raman Spectroscopy of the S₂ (1Bu) Excited State of beta-Carotene. *J. Phys. Chem. A* **2004**, *108*, 5921-5925.
- (16) McCamant, D. W.; Kukura, P.; Mathies, R. A. Femtosecond Stimulated Raman Study of Excited-State Evolution in Bacteriorhodopsin. *J. Phys. Chem. B* **2005**, *109*, 10449-10457.
- (17) Kovalenko, S. A.; Dobryakov, A. L.; Ernsting, N. P. An Efficient Setup for Femtosecond Stimulated Raman Spectroscopy. *Rev. Sci. Instrum.* **2011**, *82*, 063102.
- (18) Laimgruber, S.; Schachenmayr, H.; Schmidt, B.; Zinth, W.; Gilch, P. A Femtosecond Stimulated Raman Spectrograph for the Near Ultraviolet. *Appl. Phys. B-Lasers O.* **2006**, *85*, 557-564.
- (19) Zhu, L.; Sage, J. T.; Champion, P. M. Observation of Coherent Reaction Dynamics in Heme Proteins. *Science* **1994**, *266*, 629-632.
- (20) Kobayashi, T.; Wang, Z. Spectral Oscillation in Optical Frequency-Resolved Quantum-Beat Spectroscopy With a Few-Cycle Pulse Laser. *IEEE J. Quantum Elect.* **2008**, *44*, 1232-1241.
- (21) Liebel, M.; Schnedermann, C.; Kukura, P. Vibrationally Coherent Crossing and Coupling of Electronic States during Internal Conversion in beta-Carotene. *Phys. Rev. Lett.* **2014**, *112*, 198302.
- (22) Liebel, M.; Kukura, P. Broad-Band Impulsive Vibrational Spectroscopy of Excited Electronic States in the Time Domain. *J. Phys. Chem. Lett.* **2013**, *4*, 1358-1364.

- (23) Kraack, J. P.; Wand, A.; Buckup, T.; Motzkus, M.; Ruhman, S. Mapping Multidimensional Excited State Dynamics Using Pump-Impulsive-Vibrational-Spectroscopy and Pump-Degenerate-Four-Wave-Mixing. *Phys. Chem. Chem. Phys.* **2013**, *15*, 14487-14501.
- (24) Weigel, A.; Dobryakov, A.; Klaumünzer, B.; Sajadi, M.; Saalfrank, P.; Ernsting, N. P. Femtosecond Stimulated Raman Spectroscopy of Flavin after Optical Excitation. *J. Phys. Chem. B* **2011**, *115*, 3656-3680.
- (25) Pollard, W. T.; Mathies, R. A. Analysis of Femtosecond Dynamic Absorption Spectra of Nonstationary States. *Annu. Rev. Phys. Chem.* **1992**, *43*, 497-523.
- (26) Liebel, M.; Schnedermann, C.; Kukura, P. Sub-10-fs Pulses Tunable from 480 to 980 nm from a NOPA Pumped by an Yb:KGW Source. *Opt. Lett.* **2014**, *39*, 4112-4115.
- (27) Megerle, U.; Pugliesi, I.; Schrieffer, C.; Sailer, C. F.; Riedle, E. Sub-50 fs Broadband Absorption Spectroscopy with Tunable Excitation: Putting the Analysis of Ultrafast Molecular Dynamics on Solid Ground. *Appl. Phys. B-Lasers O.* **2009**, *96*, 215-231.
- (28) Liebel, M.; Schnedermann, C.; Bassolino, G.; Taylor, G.; Watts, A.; Kukura, P. Direct Observation of the Coherent Nuclear Response after the Absorption of a Photon. *Phys. Rev. Lett.* **2014**, *112*, 238301.
- (29) Fuciman, M.; Durchan, M.; Slouf, V.; Kesan, G.; Polivka, T. Excited-State Dynamics of Astaxanthin Aggregates. *Chem. Phys. Lett.* **2013**, *568*, 21-25.
- (30) Polivka, T.; Sundstrom, V. Ultrafast Dynamics of Carotenoid Excited States-From Solution to Natural and Artificial Systems. *Chem. Rev.* **2004**, *104*, 2021-2071.
- (31) Wand, A.; Loevsky, B.; Friedman, N.; Sheves, M.; Ruhman, S. Probing Ultrafast Photochemistry of Retinal Proteins in the Near-IR: Bacteriorhodopsin and Anabaena Sensory Rhodopsin vs Retinal Protonated Schiff Base in Solution. *J. Phys. Chem. B* **2012**, *117*, 4670-4679.
- (32) Sakamoto, A.; Tanaka, F.; Tasumi, M.; Torii, H.; Kawato, K.; Furuya, K. Comparison of the Raman Spectrum of Trans-Stilbene in the S1 State Calculated by the CIS Method and the Spectra Observed under Resonant and off-Resonant Conditions. *Vib. Spectrosc.* **2006**, *42*, 176-182.
- (33) Kovalenko, S. A.; Dobryakov, A. L. On the Excitation Wavelength Dependence and Arrhenius Behavior of Stilbene Isomerization Rates in Solution. *Chem. Phys. Lett.* **2013**, *570*, 56-60.

TOC IMAGE

